Atomic-scale simulation of 50 keV Si displacement cascades in β-SiC

F. Gao and W. J. Weber
Pacific Northwest National Laboratory, MS K8-93, P.O. Box 999, Richland, Washington 99352
(Received 27 June 2000; published 22 December 2000)

Molecular dynamics (MD) methods with a modified Tersoff potential have been used to simulate high-energy (50 keV) displacement cascades in β-SiC. The results show that the cascade lifetime is very short, 10 times shorter than that in metals, and the surviving defects are dominated by C interstitials and vacancies, which is similar to behavior for 10 keV cascades in SiC. Antisite defects are generated on both sublattices. Although the total number of antisite defects remaining at the end of the cascade is smaller than that of Frenkel pairs, the number of Si antisites is larger than the number of Si interstitials. Most surviving defects are single interstitials and vacancies, and only 19% of the interstitial population is contained in clusters. The size of the interstitial clusters is small, and the largest cluster found, among all the cascades considered, contained only four interstitial atoms, which is significantly different behavior than obtained by MD simulations in metals. It is observed that all clusters are created by a quenched-in mechanism directly from the collisional phase of the cascade to their final arrangements. The initial Si recoil traveled about 65 nm on average, generating multiple subcascades and forming a dispersed arrangement in the cascade geometry. These results suggest that in-cascade or direct-impact amorphization in SiC does not occur with any high degree of probability during the cascade lifetime of Si cascades, even with high-energy recoils, consistent with previous experimental and MD observations.

DOI: 10.1103/PhysRevB.63.054101 PACS number(s): 61.80.−x, 61.72.Ji, 71.15.Pd, 61.82.Fk

I. INTRODUCTION

Silicon carbide (SiC) offers a number of potential applications for both electron devices and structural materials involved in irradiation environments because of its outstanding physical and nuclear properties. The small cross section, low activation, and good thermal conductivity of SiC under neutron irradiation are particularly important for its potential use in structural components for fusion reactors,[1] as an inert matrix for the transmutation of plutonium[2] and as cladding material for gas-cooled fission reactors.[3] There has been a rapid growth of activity in the experimental study and the modeling of energetic-beam interactions, such as those encountered in ion-beam processing or in irradiation environments, on the structure and properties of SiC in the past few years. Although there have been numerous investigations of ion-induced damage and recovery in SiC by employing a wide range of analytical techniques (see reviews[4,5]), a complete understanding of beam-solid interactions demands computer simulations to obtain an insight into the atomic-level processes.

During the last decade, computer simulations by molecular dynamics (MD) have been employed to understand the nature of the damage produced by fast atomic particles in materials from metals[6,7] to ceramics.[8,9] In particular, these simulations provided information of not only the mechanisms that control the production of defects in displacement cascades but also the number and arrangement of the defects generated. Such knowledge is crucial for the successful development of multiscale modeling of microstructure evolution under irradiation over long periods of time, such as in kinetic Monte-Carlo methods. Although there have been previous, studies of displacement cascades in SiC,[8–10] the energy of the primary recoil atoms (PKA), E_p, has only been considered up to 10 keV, whereas the average recoil energy from a fission spectrum is on order of 50 to 300 keV and that from a fusion spectrum ranges up to 2 MeV. It is of, therefore, interest to extend the MD simulations to higher PKA energy.

Additionally, the results of irradiation experiments using ion beams[11,12] and electrons[13,14] on SiC have demonstrated that there is an irradiation-induced crystalline-to-amorphous transformation below a critical temperature, which is dependent on the irradiation conditions. Furthermore, most of the experimental results indicate that amorphization in SiC is dominated by a defect-stimulated amorphization process, which occurs from the accumulation of ion-beam-induced defects or is assisted by the overlap of damage cascades. Previous simulations of displacement cascades at low energy[8,9] have shown that direct-impact (in-cascade) amorphization does not occur due to the high-melting temperature of SiC and the small mass of the SiC system. Since the energy density in the core of cascades at higher energy may be different from that of low-energy cascades, it is necessary to simulate higher-energy cascades in order to determine the primary damage states and the mechanisms of irradiation-induced amorphization in SiC over a range of PKA energies.

In the following, the model and methods employed for the present simulations are described, and the melting temperature, T_m, is determined for the model of 3C−SiC (cubic, beta phase), which is an important parameter to understand the cascade process. The results on the evolution of 50 keV cascades and their geometrical features at the end of cascades are presented in Sec. IV. Data for the final number of defects created and the size distribution of defect clusters are analyzed in Sec. V, and other aspects of the results are discussed in Sec. VI.

II. SIMULATION MODEL AND METHOD

The MD code employed in these simulations is a modified version of MDCASK,[15] and the simulations are run on a

massively parallel Cray T3E at the National Energy Research Scientific Computing Center (NERSC) at Lawrence Berkeley National Laboratory. The code has been further modified to incorporate a subroutine to identify interstitials, vacancies, and antisite defects based on the PVM message passing library. In addition, the arrays used in MDCASK have been rearranged in order to achieve the simulation of ten million atoms. The original program was designed only for constant volume calculation, but the modified code is able to investigate cascade events under constant pressure conditions. The shape of the MD block is rectangular with dimension $60a_0 \times 60a_0 \times 210a_0$, where a_0 is the lattice parameter, such that 6 048 000 atoms were used for the 50 keV cascades. Since the MD simulation does not include energy losses due to electronic stopper power, the 50 keV of nuclear energy deposition actually corresponds to a Si PKA of about 270 keV, as determined using TRIM.[16] Periodic boundary conditions are applied in three directions, and the temperature is controlled by coupling the atoms in the four outermost planes along the cell boundaries to a reservoir of heat at 300 K. Due to the open structure of β-SiC and light masses of the SiC system, channeling occurred in most of cascades attempted. This caused the PKA and energetic recoils to cross the boundaries of the simulation box and reemerge elsewhere causing cascade overlap. In this event, the simulation is restarted choosing another Si atom near the top of the MD box. Only three 50 keV cascades have been completed out of more than twelve simulations started.

Before the primary recoil is initiated, the perfect crystal block is equilibrated for 5 ps at 300 K to achieve an equilibrium phonon state. The cascades are initiated by giving a Si atom near the top of the cell a kinetic energy of 50 keV along the [135] direction. Several other high-index directions have been tested to see if there are any effects on cascade geometry and production, but no correlation between the damage state and the PKA direction has been found. This is due to the fact that the recoil atom travels a long distance and creates multiple subcascades, independent of the original PKA direction chosen, as discussed below. The evolution of each displacement cascade is examined for about 20 ps following the primary knock-on event. Tersoff potentials[17] with cutoff distances scaled by the cell volume[18] are used to describe the interactions between atoms, where the short-range interactions have been modified to match *ab initio* calculations,[19] as described previously by Devanathen *et al.*[8] The threshold displacement energies determined using these potentials are in good agreement with those obtained by both first-principles calculations and experimental methods.[20] The vacancy formation energies are predicted to be 5.15 and 5.90 eV for the C and Si sublattices, respectively. Several configurations of self-interstitial atoms (SIA's) are found to be stable in the static lattice, and the most stable interstitial is a C-Si$\langle 100 \rangle$ dumbbell centered on Si sites with formation energy of 5.88 eV, which is in reasonable agreement with that found in recent *ab initio* calculations.[21] These results suggest that the model potentials are well suited for damage investigations in SiC.

III. MELTING IN β-SiC

As described earlier, the melting temperature is especially relevant to damage cascades with energies above 1 keV, where local melting is thought to occur. Therefore, the melting temperature, T_m, for our model is determined by calculating the $T-t$ (Temperature-time) curve for a crystal as it is heated from solid to liquid. The method used for the determination of the melting temperature is called a ''semiconstant volume simulation,'' as described by Osetsky and Serra.[22] In this method, the lattice parameters of the crystal are taken as those due to thermal expansion at the simulation temperatures. This can be done by applying the Parinello-Rahman method to a microscope perfect system.[23] To obtain melting, the crystal must be overheated by $\Delta T_m = T_{\mathrm{inst}} - T_{\mathrm{melt}}$ to achieve the desired instability, where T_{inst} is the simulation temperature corresponding to the instability of the crystal and T_m is the actual melting temperature. The smaller the value of ΔT_m and the longer the simulated time, the more accurate is the melting temperature that is determined. In the present study, the qualitative aspects of the phase instability were of interest, rather than an accurate value of T_{melt}; therefore, the simulation was limited to a time interval of about 200 ps with a constant timestep of 5×10^{-17} s. The calculational block was cubic and consisted of $10 \times 10 \times 10$ unit cells that contained 8000 atoms.

Using semiconstant conditions, the critical simulation temperature for β-SiC, T_{inst}, was determined to be about 3900 K, and melting of the crystal was observed after 40 ps. Once melting starts, the temperature decreases and mean square displacements of atoms (MSD) increases. The temporal behavior of temperature and the MSD for this simulation are shown in Figs. 1(a) and 1(b), respectively, where the MSD for C and Si atoms are plotted separately. It is noted that a few C Frenkel pairs are created at 10 ps, and their migration leds to an increase in the MSD, which creates local melting. Melting is observed at about 40 ps. At longer time, the increase in the MSD with time is almost linear, which corresponds to a diffusion process in melted SiC. It is also interesting to note that the MSD for the Si atoms remains almost constant until 45 ps. At this time, all Si atoms become unstable, and the MSD increases instantaneously. This may be related to the relative stability and mobility of the SIA's of the two atomic species, since the formation energy is generally higher for the Si interstitials in our model.

During melting, the temperature decreases with time continually due to the transfer of kinetic energy to the potential energy of system as the crystal changes from solid to liquid. After about 120 ps, the system reaches an equilibrium state, and the temperature becomes almost constant. The melting process for the whole simulation crystal takes about 80 ps, which may reflect the high latent heat required for solid-liquid transformation for β-SiC. The estimated melting temperature, T_m, is about 3050 K. This temperature should be regarded as the upper limit for melting because T_m obtained under the present study will be higher or equal to the real melting temperature for the system. However, the value of T_m that has been determined, based on the current potentials

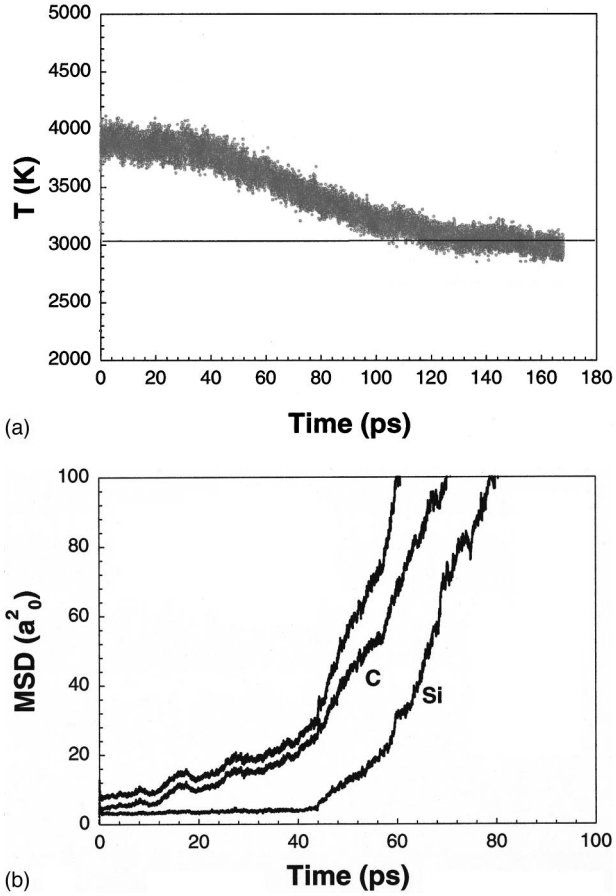

FIG. 1. The variation of (a) the mean crystallite temperature and (b) the mean-square displacement with time during semiconstant volume simulations in SiC, where the data for C and Si are also shown separately.

in this study, is in reasonable agreement with the experimental value of 2800 K.

IV. CASCADE MORPHOLOGY AND GENERATION

The peak and final damage states of a typical 50 keV cascade in SiC are shown in Figs. 2(a) and 2(b), respectively, where only displaced atoms are plotted. The interstitials are represented by large spheres and vacancies by small ones, as indicated in the legend. The vacancies are lattice sites that have no atoms within half the first-neighbor distance, and vice versa for interstitials. The 50 keV Si recoil was started near the top of the MD box, and there is a rapid build up in the number of displaced atoms during the collisional phase until a maximum in the number is reached at about 0.35 ps. During the subsequent relaxation stage, recovery due to recombination occurs, so that by about 1.1 ps most displaced atoms have become reassociated with lattice sites, and a stable state is reached. Only occasional interstitial rotation occurs at longer times. The PKA Si in this simulation atom traveled about 80 nm along the [001] direction before it came to rest in the lattice. From Figs. 2(b) and 2(c), it is clear that the PKA generates multiple branches along its path, forming distinct regions separated from each other with a low energy density in the cores of the subcascades. The final damage state of the cascade, as shown in Figs. 2(b) and 2(c), is dominated by interstitials and vacancies rather than antisite defects. This is in significant contrast to results for an ordered alloy,[24] where the dominant effect of similar cascades is the formation of a disordered zone consisting of antisites. It is interesting to note that most defects are single interstitials and monovacancies, and only a small proportion of the interstitials is found in clusters. The size of the interstitial clusters is very small. Direct inspection of the defect types indicates that the number of C interstitials is greater than that of Si interstitials, with 225 and 74 of each, respectively. This is expected because of the smaller threshold energy for C atoms in SiC system.[20] The number of Si antisite defects, C_{Si}, (i.e., C on Si lattice site) is slightly larger than that of Si_C antisites, which properly reflects the lower formation energy of the Si antisite.

In order to further characterize the evolution and nature of these cascades, the number of antisite defects and atoms displaced into interstitial positions is plotted in Fig. 3 as a function of time, where Si and C components are shown separately. The increase in the number of displaced atoms, N_d, during the collisional stage reaches a maximum at about 0.35

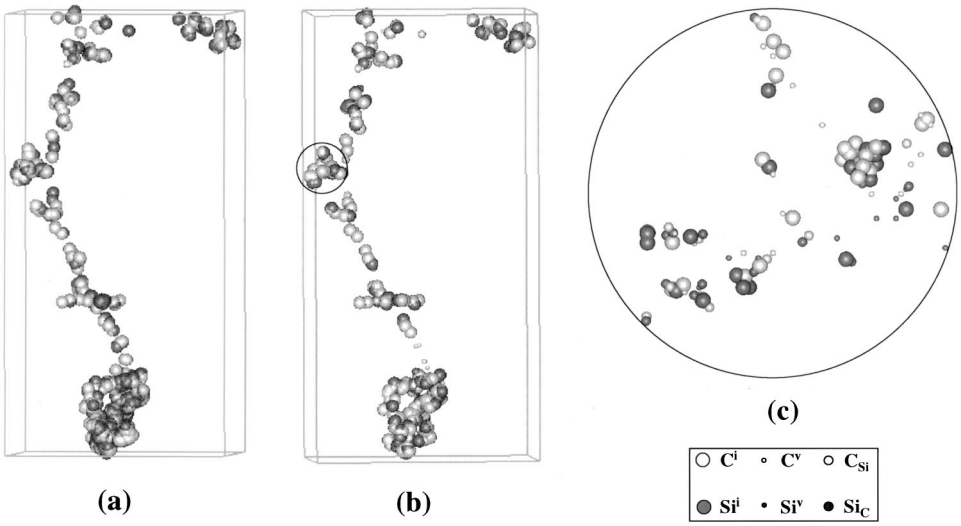

FIG. 2. Illustration of a typical 50 keV cascade in SiC at the peak damage state (a), the final damage state (b), and (c) the defect distribution in a small region indicated in the plot (b). The defect type is distinguished by size and gray.

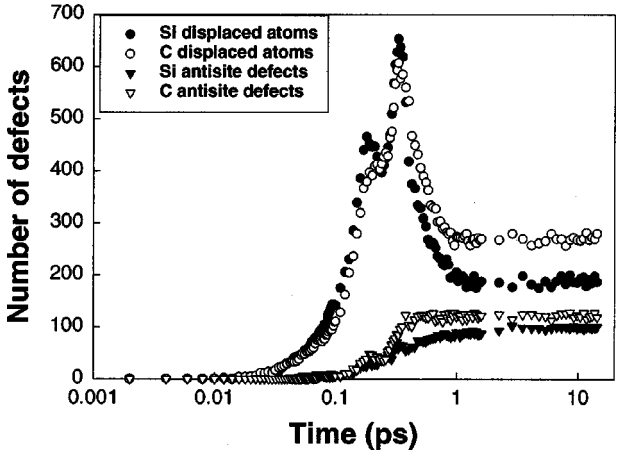

FIG. 3. The number of Si and C displaced atoms and antisite defects as a function of time in a 50 keV Si cascade in SiC.

ps, t_{peak}; after which, N_d decreases during relaxation, as expected. It is of interest to note that the number of ''interstitial'' defects decline rapidly to final values within 0.7 ps. This demonstrates that the cascade lifetime, defined as the time during which the number of defects reach to its final value, is very short in SiC, about ten times smaller than that in metals for the same or even smaller PKA recoil energies.[25] As a consequence of this, most defects are produced in the form of single interstitials and monovacancies, as shown in Fig. 2(c). Nearly 70% of the displaced Si atoms recombine with vacancies. Another interesting feature is that most antisite defects are generated during the collisional phase, when the maximum in N_d is reached, and the increase in antisite defects is very small during relaxation. This implies that the formation of antisite defects is due to replacement collision sequences, although they are very short. This is also confirmed by using a visualization package on a work station and calculating the mixing parameter Q. A mixing parameter can be obtained from the total mean square displacement (MSD) of the atoms at the end of cascade and is given by

$$Q=\sum_{i=1}^{N} r_i^2/6n_0E_P\,, \tag{1}$$

where E_p is PKA energy and n_0 is the number density of atoms. The total mean square displacement of 657.73 nm^2 yields a value of Q of about $2.3\times10^{-5}\,\text{nm}^5/\text{eV}$, which is consistent with that found in 10 keV cascades,[8] indicating a poor mixing efficiency in SiC. Furthermore, the separate mixing parameters for C and Si are calculated to be 1.12×10^{-5} and $1.15\times10^{-5}\,\text{nm}^5/\text{eV}$, respectively.

V. DEFECT PRODUCTION AND CLUSTERING

As indicated elsewhere,[7,25] the final number of defects produced in displacement cascades is an important parameter for theories and models of radiation-damage evolution. It is, therefore, of interest to calculate this parameter and to compare the value with those estimated from the standard formula of Norgett, Robison, and Torrens (NRT)[26] given by

TABLE I. The number, N_F, of Frenkel pairs and the number, N_{AS}, of antisite defects at the end of 50 keV cascades, averaged over all cascades simulated, in SiC.

	C	Si
N_F	243	76
N_{AS}	110	123

$$N_{\text{NRT}}=0.8E_{\text{dam}}/2E_d\,, \tag{2}$$

where E_{dam} is the energy of the primary recoil atom dissipated elastically in collisions and E_d is the mean threshold displacement energy. Data for the final number Frenkel pairs, N_F, and antisite defects, N_{AS}, at the end of the cascade process in SiC are listed in Table 1, averaged over all cascades simulated. As noted above, N_F for C is greater than that for Si, with 243 C and 76 Si Frenkel pairs, respectively, giving a ratio of the number of C to Si interstitials to be 3.2:1. (Note that N_F represents the true number of interstitials, for the vacant lattice site and two displaced atoms, which form an interstitial dumbbell, have been counted as one interstitial.) This is in good agreement with the ratio of 3.5:1 found in 10 keV cascades.[8] From the total number of 319 interstitials, we can deduce the efficiency of Frenkel pair production using the equation

$$k'=N_F/N_{\text{NRT}}\,, \tag{3}$$

where N_{NRT} is the standard value given by Eq. (2). By setting E_{dam} as the PKA energy in the NRT formula and taking a value for threshold energy of 25 eV suggested by experimental observations, which is close to the value obtained by computer simulations,[20] the production efficiency is about 0.32 for the 50 keV cascades considered. This has demonstrated that defect production efficiency is similar to those found in metals or alloys, even if there is the absence of a thermal spike in SiC.

The number of C antisite defects is slightly larger than that of Si antisite defects, and the total number of antisite defects is smaller than that of Frenkel pairs produced, in contrast to those found in Ni_3Al,[24] where the final state of cascade damage is dominated by antisite defects. It is interesting to note that most antisite defects are generated during relaxation in Ni_3Al, while most of them are created during the collisional phase in SiC, as described in Sec. IV. The formation of interstitial clusters within their parent cascades is an important feature in MD simulations because in-cascade clustering affects defect behavior and microstructure change and, therefore, plays an important role in subsequent evolution of irradiation damage. Data for final cluster distribution of interstitials, averaged over all the cascades, are plotted in the form of histograms in Fig. 4, together with those of 40 keV cascades simulated in α-Fe (Ref. 25) for comparison, where the nearest-neighbor criterion for clustering is applied. The striking feature of this figure is that most defects formed in SiC are single interstitials, and only a small proportion are in cluster form. The size of the interstitial clusters is very small in comparison with that found in α-Fe, and the largest cluster contains only four interstitial atoms, which is considerably different from results obtained

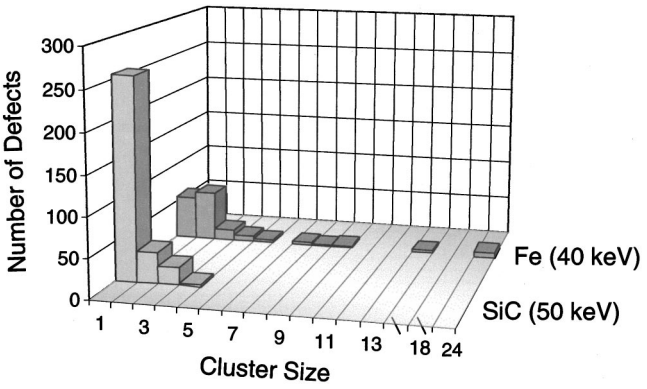

FIG. 4. Interstitial cluster size distribution for 50 keV cascades in SiC, together with the data of 40 keV cascades in α-Fe[23] for comparison.

in metals and alloys[7] in which a few tens of atoms can be found in a cluster. There are two reasons for this. First, the PKA atoms traveled a long distance and generated dispersed subcascades. The phenomenon of extensive subcascade formation in SiC may offer a physical basis for its defect production and clustering. Second, the very short lifetime of cascade prevents the short-range diffusion of atoms in the first few ps after collisional stage, which reduces the probability of forming large clusters. It was found that almost all clusters were formed directly from a quenching-in mechanism by the end of the collisional phase when groups of atoms were pushed into interstitial positions from the cascade center due to the initial shock wave. This has also been confirmed using dynamical visualizations. Furthermore, it is interesting to calculate the clustered fraction of interstitials, f_{cl}^{i}, defined as the ratio of surviving interstitials that are found in clusters of size two or more to the total number of interstitials produced in a cascade. This parameter was found to be about 0.19, much smaller than those obtained in metals. Typical values for f_{cl}^{i} are 0.58 for 40 keV cascades in α-Fe,[25] 0.53 for 10 keV cascades in Ni_3Al,[24] 0.71 for 20 keV cascades in Zr,[27] and 0.74 for 10 keV cascades in Cu.[28]

Figure 5(a) shows the crystal region containing four interstitials, where large spheres represent atoms being displaced into interstitial positions. The four interstitials cannot be interpreted as a simple structure, and are formed in a three-dimensional configuration. The small region associated with

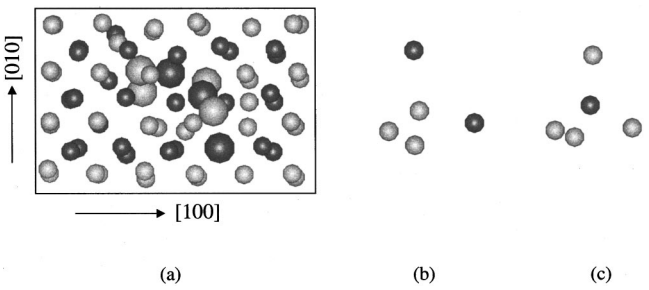

FIG. 5. The disordered region of crystal containing four interstitials produced in a 50 keV cascade (a), a C atom (black) bonding with two C and two Si atoms (b), and a Si atom (gray) with four C atoms in a tetrahedral configuration (c).

the cluster becomes disordered and loses its long-range translational order. Detailed analysis of atom positions in this region indicated that most C atoms are formed in a tetrahedral arrangement with two C and two Si atoms, as shown in Fig. 5(b). This has suggested that both C-C-C and C-Si-Si configurations can be formed after irradiation in SiC, in agreement with experimental observation.[29] The distance of C-C bonds is about 0.157 nm, which is comparable with the nearest-neighbor distance for diamond (0.155 nm). The 0.196 nm length for C-Si bonds is close to the nearest-neighbor distance (0.189 nm) in β-SiC. The angles between atoms are found to be between 96° and 130°. It is also interesting to note that most Si atoms have four C atoms as the nearest neighbors, forming tetrahedral binding as shown in Fig. 5(c). Again, the angles between bonds are distributed from 99° to 127°. These results indicate that the atomic arrangement centered at C or Si atoms forms distorted tetrahedral binding, which may be caused by antisite defects formed in the second nearest-neighbor sites. Nevertheless, it is well known that C atoms are able to form different hybrids (sp, sp^2 and sp^3), giving rise to crystals and disordered solids with a great variety of properties, whereas Si usually prefers fourfold sp^3 coordination at low temperature.

VI. DISCUSSION

The present results provide some insight into the primary damage process associated with the high-energy displacement cascades in β-SiC and address energy effects on defect production and clustering. As described in Sec. IV, the PKA atom traveled about 65 nm on average, and generates multiple subcascades, which prevents the cascades from forming compact structures of displaced atoms during the collisional phase and high-energy density in the cascade cores during the cascade lifetime. This may be due to the light masses of the SiC system and small scattering cross sections for Si or C atoms. The high melting temperature (3050 K in our model) also inhibits the development of liquidlike cascade, resulting in a very short lifetime of cascade. (In practice, it is reasonable to assume that there is no thermal-spike phase in SiC.) These features, together with the defect formation energies, provide a physical basis for defect production and clustering in SiC system. From Fig. 3, it is clear that the number of displaced Si and C atoms at t_{peak} is nearly identical, but the damage on the silicon sublattice partially recovers as the energy of the cascades is dissipated into the surrounding lattice, while the damage in the carbon sublattice does not. The number of Si atoms remaining as interstitials at the end of cascade is about three time smaller than the number of C atoms. The similar mixing parameter calculated for silicon and carbon atoms (1.12×10^{-5} and $1.15\times10^{-5}\,\mathrm{nm^5/eV}$ for Si and C, respectively) suggests that most silicon atoms are displaced very short distances from their lattice sites, and recover with them during relaxation.

As a consequence of the formation of dispersed cascades, defects are spread over the simulation box, and most interstitials remain as single defects in the final damage state. Only a small part of interstitials form in clusters with the largest size containing only four atoms, in contrast to those

found in metals and alloys.[24] There are two mechanisms corresponding to the formation of interstitial clusters. First, clusters can be created quite early on in the cascade process during the transition from the collision to thermal-spike phase, and second, they can also be formed due to defect diffusion during the thermal spike. The damage accumulation of the 500 and 1 keV cascades studied by de la Rubia *et al.*[10] in SiC have revealed that the damage microstructure is very stable, since annealing a cascade at 1300 K for 100 ps does not lead any changes in defect size and cascade morphology. This seems to be confirmed by Perlado *et al.*[9] in their annealing simulations of 5 and 10 keV cascades in β-SiC. Considering these simulations, together with the results of the present study, it is concluded that almost all interstitial clusters are generated at the early stage of cascades and then directly quenched into their final arrangements. The group of atoms pushed from cascade centers during the collision stage plays an important role in interstitial clustering in SiC. With regard to vacancies, no large clusters are observed in the present simulations, and most vacancies are monovacancies formed along the path of PKA atom or in the center of subcascades, consistent with previous observations.[8]

The early simulations of low-energy cascades[8] have shown that a very small number of antisite defects are created at the end of cascades, such that it is difficult to interpret them properly during the cascade process. For example, only 7% of the displacements lead to the formation of antisite defects in a 10 keV cascade simulated by Devanathan *et al.*,[8] giving only four C and three Si antisites at the end of the cascade. The present simulations produce a reasonable number of antisite defects to be analyzed, namely 123 C and 110 Si antisite defects. One of interesting results is that most antisite defects are created early in the cascade process, which is significantly different from those found in an intermetallic alloy of Ni_3Al.[23] In Ni_3Al, a small proportion of antisite defects were found to be produced before the thermal spike, and about 75–85 % of them were formed during the thermal-spike phase. The poor mixing calculated in Sec. IV and short replacement collision sequences during the collision phase may be associated with the production process of antisite defects in SiC. It has been proposed that the sensitivity of SiC to amorphization by irradiation may be due to the occurrence of antisite disorder.[30] From the present simulations, it is difficult to determine the role antisite defects play in amorphization of irradiated SiC. Since the total number of antisite defects produced is smaller than that of interstitial defects and damage structures are very stable, at least for the time scales of MD simulations, it is possible that the amorphization under irradiation conditions is due to the accumulation of both interstitials and antisite defects. As described above, carbon atoms can form different hybrids, and therefore, respond differently to crystallization and disordering under irradiation. The study of defect accumulation processes under cascade overlap conditions in SiC is currently underway in this laboratory.

VII. SUMMARY

Using a semiconstant volume method, the melting temperature for the present model of β-SiC has been determined to be 3050 K, in good agreement with the experimental value. This parameter, together with small masses of SiC system, affects cascade morphology, defect production and clustering. Displacement cascades produced by Si recoils with an energy of 50 keV have been simulated, and the results show that the cascade lifetime is very short, on the order of 0.7 ps, which is about 10 times smaller than that in metals and alloys. Nearly 52% of the displaced Si atoms recombine on the Si sublattice, and only 18% of them recombine on the carbon sublattice, forming C antisite defects. Although the total number of antisite defects is smaller than that of Frenkel pairs, the number of Si antisites is larger than the number of Si interstitials. The surviving defects are dominated by C interstitials and vacancies, outnumbering the corresponding Si defects by a factor of about 3, which is consistent with previous simulations of 10 keV cascades.

The formation of multiple subcascades prevents the development of compact cascades, resulting in small number and size of defect clusters. The largest interstitial cluster contains only 4 atoms, in contrast with much larger ones found in metals and alloys. All interstitial clusters are generated at the early stage of cascades and then directly quenched into their final arrangements due to the very short lifetime of cascade. The present high-energy cascades have confirmed that the amorphization in SiC due to self atom recoils does not occur during the cascade lifetime.

ACKNOWLEDGMENTS

This research was supported by the Division of Materials Science, Office of Basic Energy Sciences, U.S. Department of Energy under Contract No. DE-AC06-76RLO 1830. The simulations were performed at the National Energy Research Scientific Computing Center, which is supported by the Office of Science, U.S. Department of Energy.

[1] P. Fenici, A. J. F. Rebelo, R. H. Jones, A. Kohyama, and L. L. Snead, J. Nucl. Mater. **258**, 215 (1998).

[2] R. A. Verrall, M. D. Vlajic, and V. D. Krstic, J. Nucl. Mater. **274**, 54 (1999).

[3] J. C. Zink, Power Eng. **10**, 1 (1998).

[4] E. Wendler, A. Helt, and W. Wesch, Nucl. Instrum. Methods Phys. Res. B **141**, 105 (1998).

[5] W. J. Weber, N. Yu, L. M. Wang, and N. J. Hess, Mater. Sci. Eng., A **253**, 62 (1998).

[6] D. J. Bacon and T. Diaz de la Rubia, J. Nucl. Mater. **216**, 275 (1994).

[7] D. J. Bacon, F. Gao, and Yu. N. Osetsky, J. Nucl. Mater. **276**, 1 (2000).

[8] R. Devanathan, W. J. Weber, and T. Diaz de la Rubia, Nucl.

Instrum. Methods Phys. Res. B **141**, 118 (1998).
[9] J. M. Perlado, L. Malerba, A. Sanchez-Rubio, and T. Diaz de la Rubia, J. Nucl. Mater. **276**, 235 (2000).
[10] T. Diaz de la Rubia, J. M. Perlado and M. Tobin, J. Nucl. Mater. **233–237**, 1096 (1996).
[11] W. J. Weber, L. M. Wang, and N. Yu, Nucl. Instrum. Methods Phys. Res. B **116**, 322 (1996).
[12] W. J. Weber and N. Yu, Nucl. Instrum. Methods Phys. Res. B **127&128**, 191 (1997).
[13] H. Inui, H. Mori, and H. Fujita, Philos. Mag. B **61**, 107 (1990).
[14] H. Inui, H. Mori, and T. Sakata, Philos. Mag. B **66**, 737 (1992).
[15] T. Diaz de la Rubia and M. W. Guinan, J. Nucl. Mater. **174**, 151 (1990).
[16] J. F. Ziegler, J. P. Biersack, and U. Littmark, *The Stopping and Range of Ions in Solids* (Pergamon, Oxford, 1985).
[17] J. Tersoff, Phys. Rev. Lett. **64**, 1757 (1990); Phys. Rev. B **49**, 16 349 (1994).
[18] M. Tang and S. Yip, Phys. Rev. B **52**, 15 150 (1994).
[19] K. Nordland, J. Keinonen, and T. Mattila, Phys. Rev. Lett. **77**, 699 (1996).
[20] R. Devanathan and W. J. Weber, J. Nucl. Mater. **278**, 258 (2000).
[21] F. Gao, E. J. Bylaska, W. J. Weber, and L. R. Corrales, Nucl. Instrum. Methods Phys. Res. B (to be published).
[22] Yu. N. Osetsky and A. Serra, Phys. Rev. B **57**, 755 (1998).
[23] M. Rarrinelo and A. Rahman, Phys. Rev. Lett. **45**, 1196 (1980).
[24] F. Gao and D. J. Bacon, Philos. Mag. A **71**, 43 (1995).
[25] D. J. Bacon, F. Gao, and Yu. N. Osetsky, Nucl. Instrum. Methods Phys. Res. B **153**, 87 (1999).
[26] M. J. Norgett, M. T. Robinson, and I. M. Torrens, Nucl. Eng. Des. **33**, 50 (1975).
[27] S. J. Wooding, L. M. How, F. Gao, A. F. Calder, and D. J. Bacon, J. Nucl. Mater. **254**, 191 (1998).
[28] W. J. Phythian, A. J. E. Foreman, R. E. Stoller, D. J. Bacon, and A. F. Calder, J. Nucl. Mater. **223**, 245 (1995).
[29] W. Bolse, Nucl. Instrum. Methods Phys. Res. B **148**, 83 (1999).
[30] L. W. Hobbs, A. N. Sreeram, C. E. Jesurum, and B. A. Berger, Nucl. Instrum. Methods Phys. Res. B **116**, 18 (1996).